*Proceedings of the International Conference on Biomedical Engineering and Systems*
*Prague, Czech Republic, August 14-15, 2014*
*Paper No. 70*

# Effect of Flow-diverter Stent on In Vitro Aneurysmal Flow

**Pascal Corso, Simone Gremmo, Grégory Coussement**
University of Mons, Faculty of Engineering, Department of Fluids-Machines
53 rue du Joncquois, Mons, Belgium
pascal.corso@umons.ac.be; simone.gremmo@umons.ac.be; gregory.coussement@umons.ac.be

***Abstract*** –The study of the intraaneurysmal flow modifications due to the use of flow diverting devices such as wire-braided stents is a subject of interest for patients, physicians and stent manufacturing companies. In fact, the necessity of preventing the cerebral aneurysm ruptures and the minimally invasive technique that Flow-Diverter stents represent lead the researchers to improve the tools implemented to demonstrate the benefits of stenting an aneurysm. This work has been carried out in two parts. One part characterizes the flow changes caused by the insertion of a stent using the Particle image velocimetry technique. The other part consists in comparing the experimental results with numerical results and highlight thereby the causes of the differences observed.
For that purpose, a wire-braided stent made by the Belgian company Cardiatis was inserted inside a silicone model of an intracranial aneurysm. Different steady flow rates were applied using a peristaltic pump and a mix of water and glycerine was used to get closer to the dynamic viscosity of blood. Particle Image velocimetry technique was applied to measure experimentally the velocity fields inside the aneurysm model which were compared with numerical results. The flow patterns for the non-stented and stented configurations were observed and the velocity values were at least six times less in the stented case than in the non-stented case. In addition, the comparison between experimental and numerical results showed some discrepancies which were explained by the approximations made for both experimental and numerical parts. The present results and discussion will be useful for a further comprehensive matching between experiments and numerical simulations in order to characterize the effect of Flow-Diverters on hemodynamics. This will lead to a better design of stents and a wider awareness of the key issues for numerical simulations.

***Keywords*****:** Flow-Diverter stent, Particle image velocimetry, Intracranial aneurysm, Numerical simulations.

## 1. Introduction

Intracranial aneurysms consist in a progressive and permanent bulging of a cerebral artery. They are generally formed at the level of the Circle of Willis and, due to the presence of peculiar flow patterns and connected physiological mechanotransduction responses (as shown by Salsac, 2005), can lead to the rupture of the aneurysm wall. This rupture results in subarachnoid hemorrhage (SAH) associated with a high mortality rate. Therefore, preventing this rupture is of major interest. The use of an endovascular prosthesis known as a Flow-Diverter or Flow-Modulator stent has been shown as a promising way to prevent the growth of the aneurysm and its subsequent rupture (Berge et al., 2012).

The main purpose of the study carried out is to characterize the influence of an endovascular stent made by Cardiatis[1] (Web-1) on the aneurysmal flow within a silicone model of cerebral aneurysm using a 2D2C PIV (Particle Image Velocimetry) device. In order to complement the experimental study, the PIV results are compared with numerical simulations performed under the same steady conditions. Hence a quality analysis of the results based on the discrepancies observed between experimental and numerical results will enable us to point out the key changes to operate with the aim of improving both approaches.

[1] Cardiatis is a Belgian company which designs and manufactures multilayer wire-braided stents for the treatment of cardiovascular diseases.

## 2. Setup

The experimental setup is divided into two parts namely the PIV device and the hydraulic steering system.

In regard to the PIV device, we have first a New Wave Research Solo PIV Nd-YAG laser from DANTEC Dynamics industries (Web-2) comprising two pulsed lasers, the related optical device, the power supply, the control panel and the water cooling system. Moreover, the device includes a CCD camera FlowSense 1600 x 1186 pixels from DANTEC Dynamics Company. Finally, a control computer and a synchronization unit deal with the synchronization between the laser pulses and the recording of the image frames on the CCD camera but also with the post-processing of the data thanks to the FlowMap Processor.

As far as the hydraulic steering system is concerned, the experimental materials consist of a silicone sidewall aneurysm model (see Fig. 1) in a Plexiglas box filled with glycerine, a peristaltic pump enabling the flow of the fluid, a reservoir with a mix of water (volume: 66%) and glycerine (volume: 33%). Note that the volume percentages given are set so that the mix dynamic viscosity and density respectively amount to a constant value of 3.45 Pa.s and 1090 kg/m³ at ambient temperature. We add tracer particles of guanine (Faure, 1999) to perform the measurements and a magnetic stirrer was dropped into the reservoir to have a uniform repartition of the seeding particles within the fluid. A water column enabling to dampen the flow fluctuations due to the peristaltic pump[2] and a Sistrans MAGFLO 6000 electromagnetic flow meter.

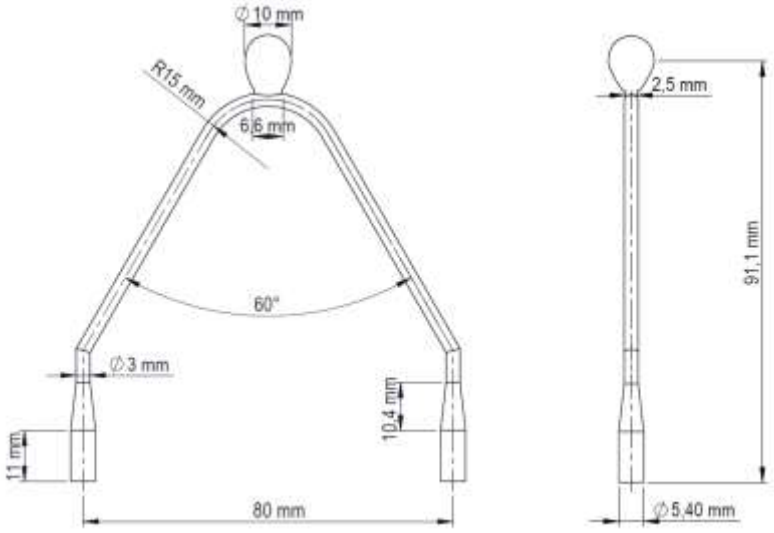


Fig. 1. Inside wall dimensions of the silicone model.

## 3. Experimental Results

PIV measurements on the aneurysm silicone model enabled us to visualize qualitatively the flow patterns with and without the Flow-Diverter but also to measure quantitatively the hemodynamical changes, namely the impact of the placement of the stent on flow quantities (velocity, vorticity, shear stresses[3]).

[2] The insertion of a water column enables also to remove from the hydraulic circuit air bubbles which bring noise to PIV measurements.

[3] Shear stresses for a Newtonian fluid such as the glycerine-water mixture and laminar flow can be calculated in bi-dimensional space with the equation: $\tau = -\mu\left(\frac{\partial u}{\partial y} + \frac{\partial v}{\partial x}\right)$.

### 3.1. Flow Patterns

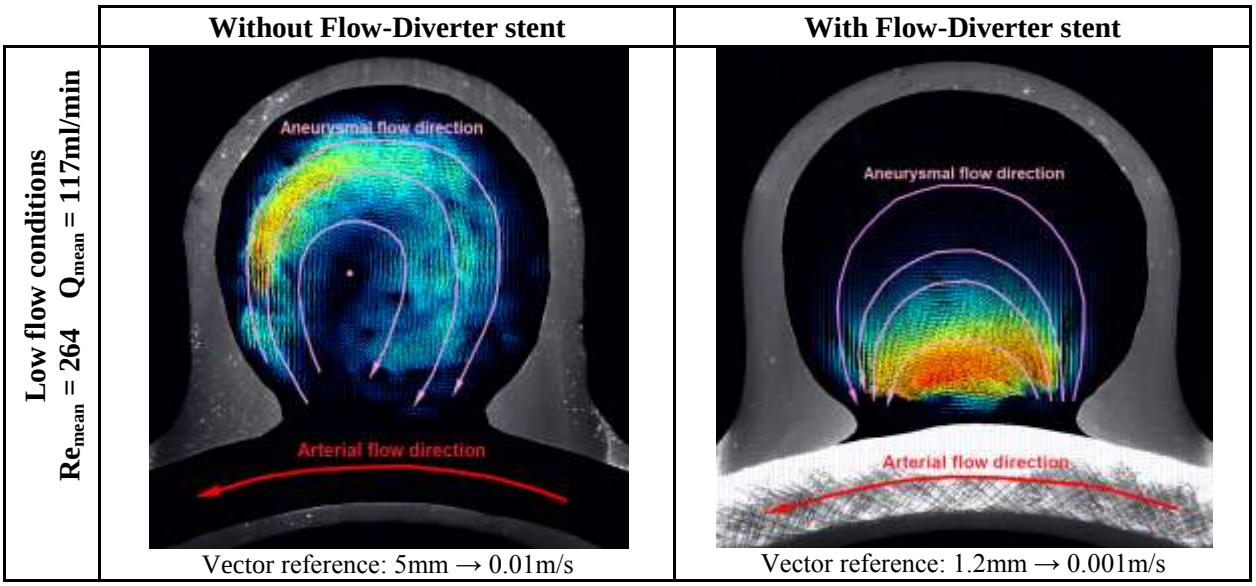


Fig. 2. PIV velocity vectors fields inside the aneurysm model with and without stent.

From the vector fields above, we can notice an inversion of the intraaneurysmal flow direction between the configurations with and without the Flow-Diverter stent. We can also see that the vortex centre moves from the aneurysm centre to the dome as the inflow increases.

### 3.2. Quantitative Results

Thanks to a post-processing analysis sequence, we can obtain the velocity values inside the aneurysm silicone model for different inflow conditions. From these velocity values, other quantities of interest such as vorticity and shear stresses can be deduced (see Table below).

*Averaged flow quantities*

Table 1. Mean aneurysmal velocity, root mean square vorticity and mean aneurysmal shear stress with and without stent and for two different flow rates.

| Configuration | Porosity $\phi$ | Vessel flow rate [ml/min] | Vessel Reynolds number | Mean velocity in the aneurysmal sac [mm/s] | RMS vorticity in the aneurysmal sac | Mean shear stress in the aneurysmal sac [Pa] |
|---|---|---|---|---|---|---|
| Without stent | 100% | 117<br>255 | 264<br>574 | **3.17**<br>**9.98** | **1.27**<br>**4.18** | **$2.36\ 10^{-8}$**<br>**$1.44\ 10^{-7}$** |
| With stent | 70% | 117<br>255 | 264<br>574 | **0.23**<br>**0.865** | **0.38**<br>**1.32** | **$7.8\ 10^{-11}$**<br>**$1.61\ 10^{-9}$** |

*Three-dimensional velocity representations*

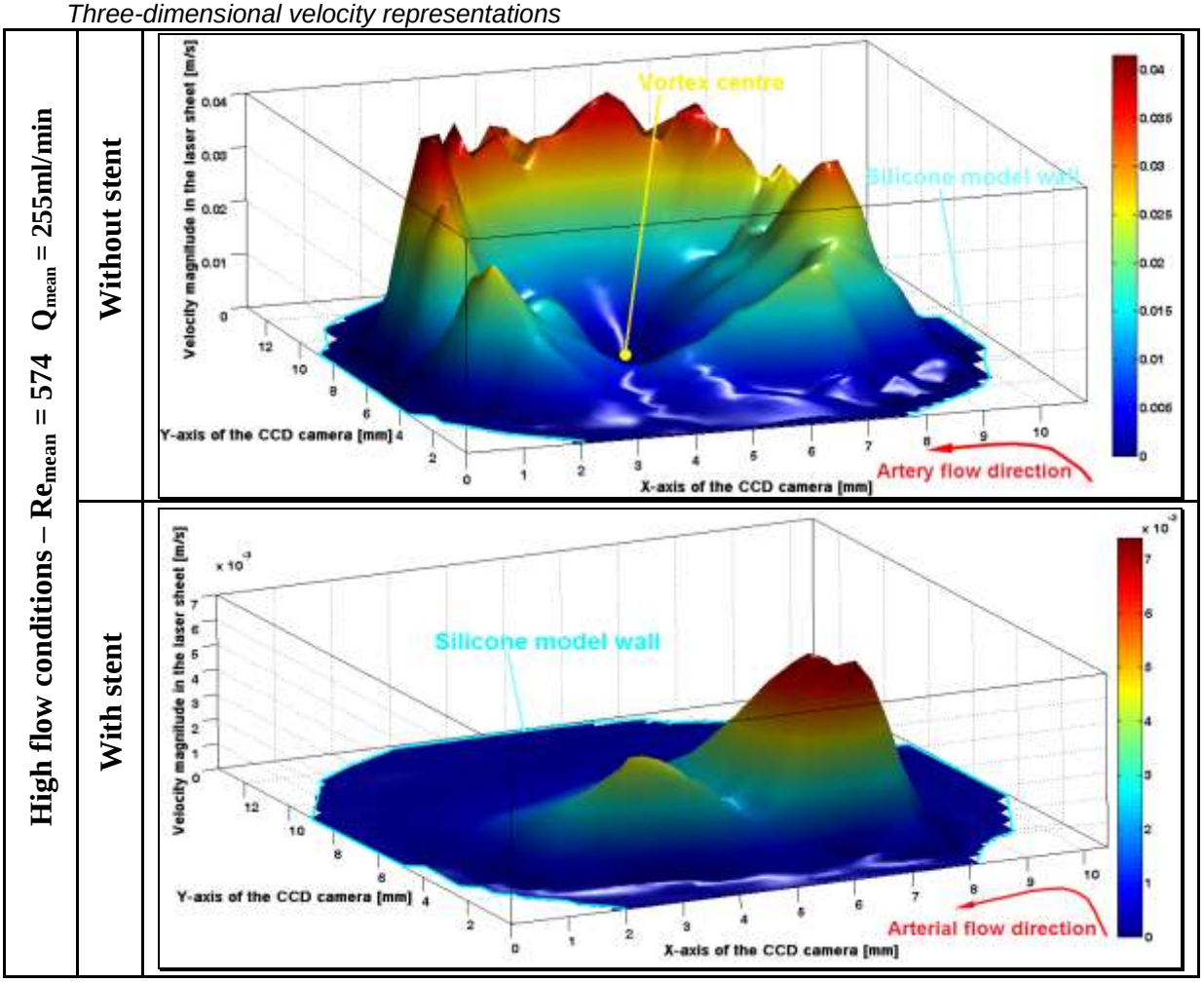


Fig. 3. Experimental velocities inside the aneurysmal sac for a vessel flow rates of 255ml/min.

From the table and graphs above, we can see that the placement of the stent for both inflows reverses the entrance direction of the flow inside the aneurysm model and decreases the velocity and subsequently the vorticity and shear stresses. Indeed, we can see on Fig. 3 that the vortex centre is no longer observable and that the velocity magnitude scale of the stented configuration varies from one sixth (high inflow conditions) to one eighth (low inflow conditions) of that of the non-stented configuration. Furthermore, as far as the quality of the results is concerned, we can note that there are some irregularities in velocity magnitude values mostly for the non-stented cases. These irregularities depend on the CCD camera resolution.

## 4. Comparison between Experimental and Numerical Results and Discussion

The quantitative results achieved thanks to PIV measurements were compared with the numerical results obtained through the implementation of the finite element method on the CAD representation of the sidewall aneurysm model. COMSOL *Multiphysics* (Web-3) was the CFD software used to perform the finite elements (FE) calculations.

For the sake of comparing the experimental and numerical results, an averaging of the numerical results on a 5mm thickness plane was performed. Indeed, the laser sheet is 5mm thick and cut the aneurysm silicone model near its midplane along the vessel axis.

In order to take into account the stent geometry in the simulations, the use of the "Free and Porous Media Flow" model from COMSOL was considered. The latter uses Brinkman's law which adds a source

term to the momentum equations. The parameters associated to this model are the porosity $\phi$ and permeability $K$ of the Flow-Diverter. As shown by Augsburger et al. (2009), the effective porosity is given by:

$$\phi = \frac{A_{free}}{A_{total}} = 1 - \frac{A_{device}}{A_{total}} \quad (1)$$

As previously shown (Koponen et al., 1998), the empirical relation giving the permeability for a three-dimensional random fibre webs is:

$$\frac{K}{r_f^2} = \frac{A}{e^{B(1-\phi)-1}} \quad (2)$$

with $r_f$ the wire radius and A, B two constants

### 4.1. Numerical Velocity Vectors

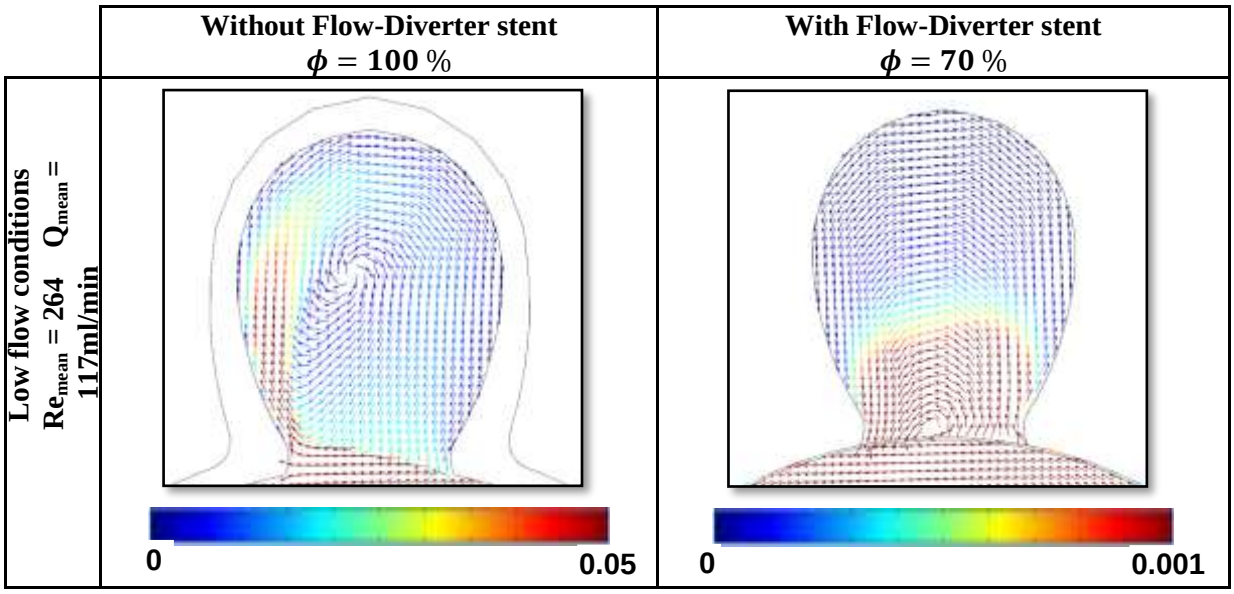


Fig. 4. Numerical flow vectors in the aneurysm model with and without stent.

The numerical intraaneurysmal velocity vectors above have similar directions as experimental vectors (see Fig. 2). We also observe the vortex centre moving towards the aneurysmal dome for non-stented configuration.

In addition, we notice that, near the stent, a vortex is present. This observation was not possible for PIV vector fields since, due to the reflection of the laser sheet on stent wires, a blowing effect prevented us from making measurements in the around stent area.

Finally, the maximum numerical velocity magnitudes without stent are greater than the maximum experimental velocity magnitudes (see Fig. 3) while the maximum numerical velocity magnitudes with stent are either lower (for the low flow conditions) or slightly greater (for the high flow conditions) than those obtained through PIV measurements.

## 4.2. Velocity Profiles

*Velocity profiles without stent*

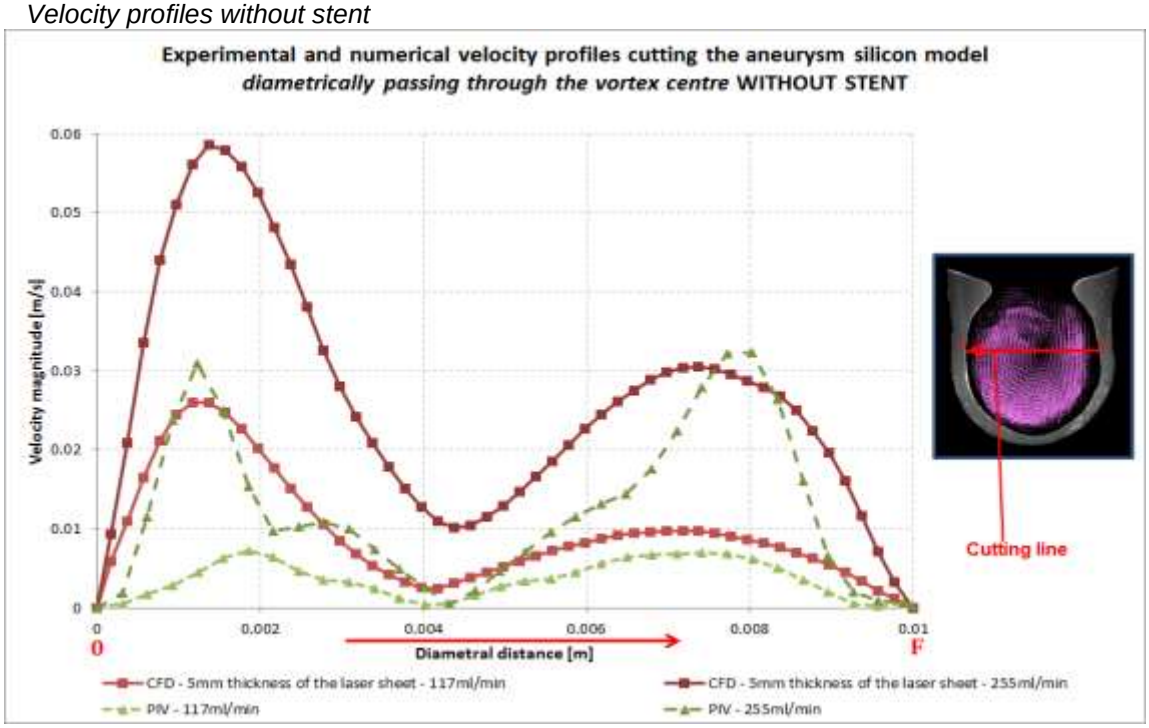


Fig. 5. Experimental and CFD velocity profiles comparison without stent for two flow rates of 117ml/min and 255ml/min.

We notice at once that the profiles seem similar in shape but that there are differences in velocity magnitude values. In fact, PIV velocities are smaller than numerical velocities in spite of the 5mm averaging performed on COMSOL.

*Velocity profiles with stent*

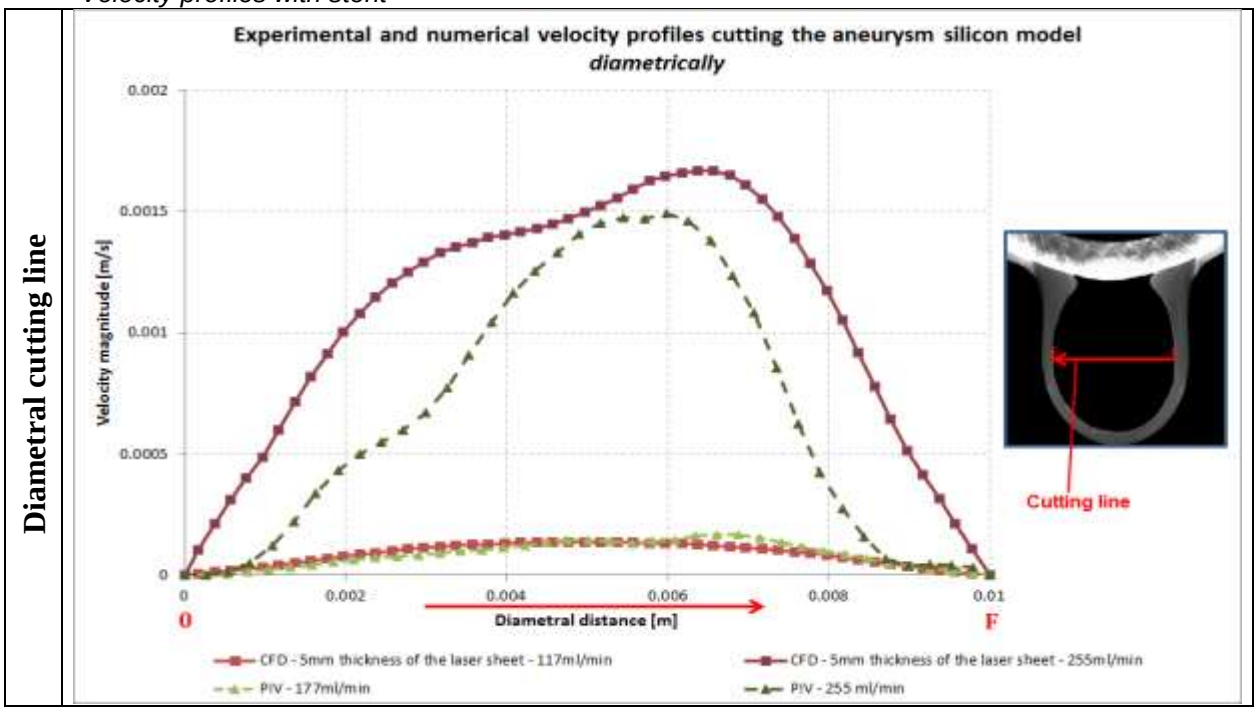

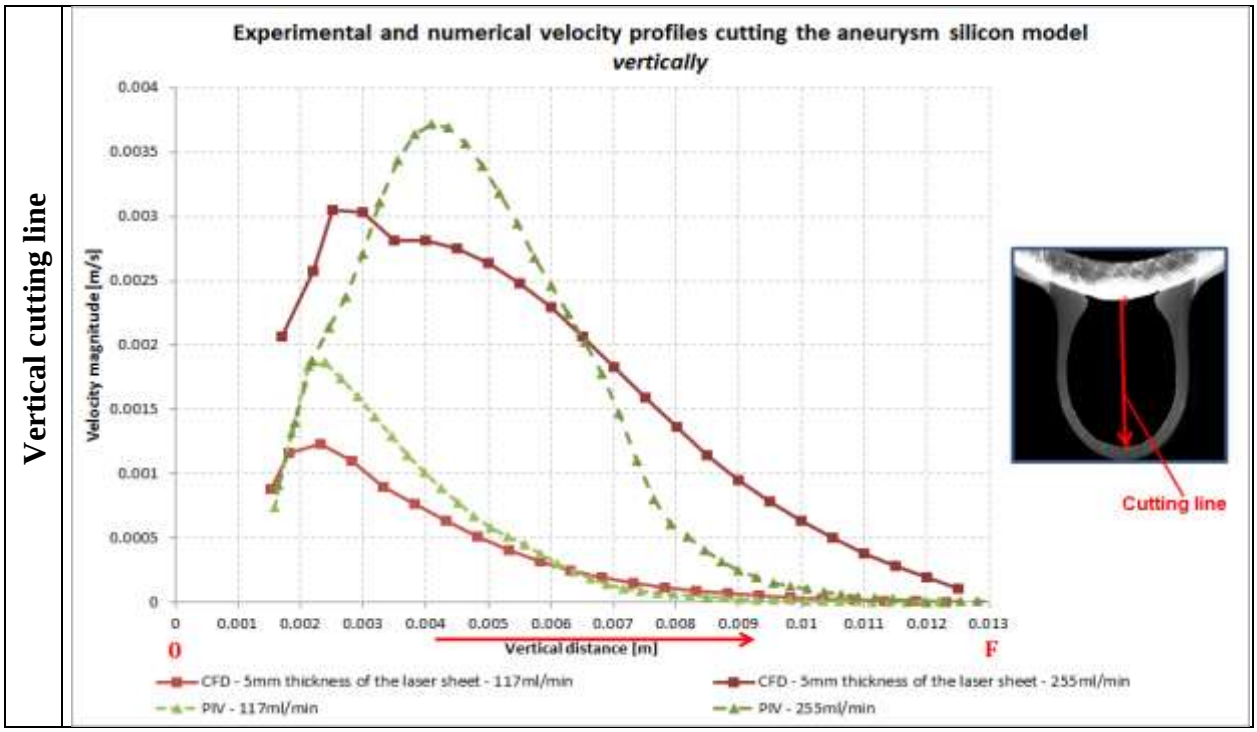


Fig. 6. Experimental and CFD velocity profiles comparison with stent for two flow rates of 117ml/min and 255ml/min.

As mentioned supra, we notice that the experimental velocity magnitude values for vertical cutting line profiles with stent insertion are predominantly greater than the numerical velocities. On the contrary, for the profiles achieved with the diametral cutting line, the PIV velocity values are lower than the numerical velocity values. On the whole, the velocity profiles have a similar look in accordance with the conclusions drawn for the comparison of the numerical and experimental flow patterns.

### 4.3. Explanation of the Differences between Numerical and Experimental Results

With regard to the experiments carried out, there are sundry imprecisions, namely:

First, the use of a peristaltic pump notwithstanding the insertion of a water damping column is a source of small flow fluctuations that are not taken into account in the steady numerical simulations.

Then, we have the uncertainty on the cutting position of the laser plan in the aneurysm silicone model.

The thickness of the laser sheet also deteriorates the accuracy due to the small dimensions of the aneurysmal sac.

Furthermore, the unavoidable experimental precision errors for measuring the volume of water and glycerine in order to have the correct density and dynamic viscosity lead to a loss of precision.

All the noise such as bubbles in the hydraulic circuit, blowing effects due to the reflection of the laser sheet on the silicone wall, on the stent or on the Plexiglas box, are detrimental to the accuracy of the results.

Concerning the incertitude for the numerical simulations, we have:

The porosity value of the stent was evaluated by a reverse process consisting in fitting the numerical results with the experimental results performed with an inlet vessel flow rate of 150ml/min. We use an empirical law giving the permeability for three-dimensional random fibre webs according to the stent wire radius and porosity to calculate stent permeability. Moreover, the anisotropy of the stent porosity and permeability when deployed into the model was not taken into account since the model implemented under COMSOL does not deal with it.

Finally, the difficulty of positioning the laser plan experimentally implies an uncertainty on the 5mm averaging performed in the numerical simulations.

## 5. Conclusion

Improving stent efficiency and reliability is one of the greatest issues for researchers, engineers, physicians and patients. For this purpose, the complementarity between the experimental and numerical studies has proved to be an appropriate strategy.

In this research, the experimental study with PIV system complemented by numerical simulations has shown the impact of inserting a stent on velocity, vorticity and shear stress values. The quality of the PIV results has been studied by comparing velocity magnitude profiles in the aneurysmal sac. The similarities in flow patterns and in the influence of stent placement between experimental and numerical results have shown the potentiality of both parts. Moreover, an analysis of the uncertainties and imprecisions related to PIV measurements and numerical models implementation enabled us to highlight the potential improvements for further investigations.


### Acknowledgements

This work was supported by the Cardiatis company regarding the endovascular device tested.

The authors also wish to warmly thank the technicians from Fluids-Machines department and all the people involved in this work.


### Conflict of Interest Statement

The authors declare that there is no actual or potential conflict of interest in relation to this paper.

## References


Augsburger L., Farhat M., Reymond Ph., Fonck E., Kulcar Z., Stergiopoulos N., Rüfenacht D. A. (2009). Effect of Flow Diverter Porosity on Intraaneurysmal Blood Flow, Clinical Neuroradiology.

Berge J., Biondi A., Machi P., Brunel H., Pierot L., Gabrillargues J., Kadziolka K., Barreau X., Dousset V., Bonafé A. (2012). Flow-Diverter Silk Stent for the Treatment of Intracranial Aneurysms: 1-year Follow-Up in a Multicenter Study, Am. J. of Neuroradiol., 33, 1150-1155.

Faure Th. (1999). Méthodes expérimentales et méthodes de visualisation en mécanique des fluides, course for Master of Advanced Study in power generation and aircraft propulsion, Université Pierre et Marie Curie, France.

Formaggia L., Quarteroni A., Veneziani A. (2009). "Cardiovascular Mathematics – Modelling and simulation of the circulatory system" Springer.

Koponen A., Kandhai D., Hellén E., Alava M., Hoekstra A., Kataja M., Niskanen K., Sloot P., Timonen J. (1998). Permeability of Three-Dimensional Random Fiber Webs, Physical Review Letters, vol.80 nb.4, 716-719.

Salsac A.-V. (2005). Changes in the Hemodynamic Stresses Occurring During the Enlargement of Abdominal Aortic Aneurysm. Ph.D. Thesis, University of California, San Diego.

Scarano F., Riethmuller M. L. (2009) Recent advances in particle image velocimetry. VKI Lecture Series. Rhode-Saint-Genèse, Belgium.

Waite L., Fine J. (2007). "Applied Biofluid Mechanics" the McGraw-Hill Companies, Inc.

Wiebers D.O., Whisnaut J.P., Huston J., Meissner I., Brown R.D., Piepgras D.G., Forbes G.S., Thielen K., Nichols D., O'Fallon W.M., Peacock J., Jaeger L., Kassell N.F., Kongable-Beckman G.L., Torner J.C. (2003). Unruptured intracranial aneurysms: Natural history, clinical outcome, and risks of surgical and endovascular treatment. Lancet, vol. 362, 103-110.

Web sites:

Web-1: http://www.cardiatis.com/ consulted 04 Sept. 2013.

Web-2: http://www.dantecdynamics.com/ consulted 22 Feb. 2014.

Web-3: http://www.comsol.com/ consulted 14 Aug. 2013.